

See discussions, stats, and author profiles for this publication at: <https://www.researchgate.net/publication/231524578>

# Reactivity of Platinum–Oxygen Bonds: Kinetic and Mechanistic Studies of the Carbonylation of Platinum Aryloxy Complexes and the Formation of (Aryloxy)carbonyls

ARTICLE in JOURNAL OF THE AMERICAN CHEMICAL SOCIETY · MAY 1996

Impact Factor: 12.11 · DOI: 10.1021/ja952680p

---

CITATIONS

43

---

READS

17

3 AUTHORS, INCLUDING:



Phillip E. Fanwick

Purdue University

639 PUBLICATIONS 11,038 CITATIONS

SEE PROFILE



Clifford P. Kubiak

University of California, San Diego

246 PUBLICATIONS 8,453 CITATIONS

SEE PROFILE

# Reactivity of Platinum–Oxygen Bonds: Kinetic and Mechanistic Studies of the Carbonylation of Platinum Aryloxy Complexes and the Formation of (Aryloxy)carbonyls

David W. Dockter,<sup>‡</sup> Phillip E. Fanwick,<sup>†</sup> and Clifford P. Kubiak\*

Contribution from 1393 Brown Laboratory of Chemistry, Department of Chemistry, Purdue University, West Lafayette, Indiana 47907

Received August 7, 1995. Revised Manuscript Received November 21, 1995<sup>⊗</sup>

**Abstract:** The reactions of [Pt(triphos)(Cl)](Cl) (**1**) {triphos = bis[2-(diphenylphosphino)ethyl]phenylphosphine} with NaOC<sub>6</sub>H<sub>4</sub>-*p*-R, in the presence of NaPF<sub>6</sub>, yields the aryloxy complexes [Pt(triphos)(OC<sub>6</sub>H<sub>4</sub>-*p*-R)](PF<sub>6</sub>) (R = OMe (**2a**), Me (**2b**), H (**2c**), F (**2d**), Cl (**2e**)). Upon reaction of **2a–e** with carbon monoxide at pressures from 10 to 134 psi in acetonitrile the (aryloxy)carbonyl complexes [Pt(triphos)(C(O)OC<sub>6</sub>H<sub>4</sub>-*p*-R)](PF<sub>6</sub>) (**3a–e**) were obtained. The molecular structure of [Pt(triphos)(C(O)OC<sub>6</sub>H<sub>4</sub>-*p*-Me)](PF<sub>6</sub>) (**3b**) was determined by X-ray diffraction. Complex **3b** crystallized in the monoclinic space group *P*2<sub>1</sub>/*n* (no. 14) with *a* = 10.797(1) Å, *b* = 19.927(3) Å, *c* = 19.113(2) Å, β = 98.07(1)°, *V* = 4071(2) Å<sup>3</sup>, and *Z* = 4. The structure was solved and refined to *R* = 0.035 and *R*<sub>w</sub> = 0.040 for 3958 reflections with *I* > 3σ(*I*). The kinetics of the carbonylation of **2a–e** to form **3a–e** were studied by <sup>31</sup>P{<sup>1</sup>H} NMR. Rates of carbonylation exhibit a first order dependence on [CO], but are independent of the concentration of free aryloxy in solution. Rates of aryloxy ligand exchange were also found to be significantly faster than rates of carbonylation. The rates of carbonylation depend on the *para*-substituent of the aryloxy ligand and follow the order F (**2d**) > Me (**2b**) > OMe (**2a**). These observations are interpreted in terms of a carbonylation mechanism that proceeds via a migratory insertion pathway, rather than by nucleophilic attack at coordinated carbon monoxide by free or dissociated aryloxy.

## Introduction

We report synthetic and mechanistic studies of platinum aryloxy and (aryloxy)carbonyl complexes. The chemistry of late transition metal aryloxides was once considered to be limited by the incompatibility of the “hard” basic ligands and “soft” metal centers.<sup>1–3</sup> In the wake of the earlier development of metal alkyl chemistry, there now exists a growing body of research on such complexes.<sup>4,5</sup> While a significant number of examples of late transition metal alkoxy complexes now exist in the literature,<sup>6–25</sup> the chemistry of late transition metal aryloxy

complexes has been slower to develop.<sup>9,11,16,21,23,26–36</sup> Bercaw and Bryndza *et al.* have shown that homolytic Pt–OR bond

<sup>†</sup> To whom correspondence pertaining to crystallographic studies should be addressed.

<sup>‡</sup> Present address: Corporate Technology, Phillips Petroleum Co., Bartlesville, OK 74004.

⊗ Abstract published in *Advance ACS Abstracts*, May 1, 1996.

- (1) Pearson, R. G. *J. Am. Chem. Soc.* **1963**, *85*, 3533.
- (2) Pearson, R. G. *J. Chem. Educ.* **1968**, *45*, 643.
- (3) Hartley, F. R. *The Chemistry of Platinum and Palladium*; Halsted Press: New York, 1973; p 169.
- (4) Bryndza, H. E.; Domaille, P. J.; Tam, W.; Fong, L. K.; Paciello, R. A.; Bercaw, J. E. *Polyhedron* **1988**, *7*, 1441–52.
- (5) Bryndza, H. E.; Tam, W. *Chem. Rev.* **1988**, *88*, 1163–88.
- (6) Sen, A.; Chen, J.-T.; Vetter, W. M.; Whittle, R. R. *J. Am. Chem. Soc.* **1987**, *109*, 148–156.
- (7) Kubota, M.; Sly, W. G.; Santarsiero, B. D.; Clifton, M. S.; Kuo, L. *Organometallics* **1987**, *6*, 1257–1259.
- (8) Bellon, P. L.; Manassero, M.; Porta, F.; Sansoni, M. *J. Organomet. Chem.* **1974**, *80*, 139–145.
- (9) Osakada, K.; Kim, Y.-J.; Yamamoto, A. *J. Organomet. Chem.* **1990**, *382*, 303.
- (10) Lunder, D. M.; Lobkovsky, E. B.; Streib, W. E.; Caulton, K. G. *J. Am. Chem. Soc.* **1991**, *113*, 1937–1938.
- (11) Kim, Y. J.; Osakada, K.; Takenaka, A.; Yamamoto, A. *J. Am. Chem. Soc.* **1990**, *112*, 1096–104.
- (12) Bryndza, H. E.; Calabrese, J. C.; Wreford, S. S. *Organometallics* **1984**, *3*, 1603–4.
- (13) Bryndza, H. E.; Calabrese, J. C.; Marsi, M.; Roe, D. C.; Tam, W.; Bercaw, J. E. *J. Am. Chem. Soc.* **1986**, *108*, 4805–13.
- (14) Bryndza, H. E.; Kretschmar, S. A.; Tulip, T. H. *J. Chem. Soc., Chem. Commun.* **1985**, *14*, 977–8.

(15) Milstein, D.; Calabrese, J. C.; Williams, I. D. *J. Am. Chem. Soc.* **1986**, *108*, 6387–6389.

(16) Alsters, P. L.; Baesjou, P. J.; Janssen, M. D.; Kooijman, H.; Sicherer-Roetman, A.; Spek, A. L.; Koten, G. v. *Organometallics* **1992**, *11*, 4124–4135.

(17) Glueck, D. S.; Winslow, L. J. N.; Bergman, R. G. *Organometallics* **1991**, *10*, 1462–79.

(18) Andrews, M. A.; Gould, G. L. *Organometallics* **1991**, *10*, 387–9.

(19) Lunder, D. M.; Lobkovsky, E. B.; Streib, W. E.; Caulton, K. G. *J. Am. Chem. Soc.* **1991**, *113*, 1937–1938.

(20) Osakada, K.; Kim, Y.-J.; Tanaka, M.; Ishiguro, S.-i.; Ohshiro, K.; Yamamoto, A. *Inorg. Chem.* **1991**, *30*, 197–200.

(21) Mandal, S. K.; Ho, D. M.; Orchin, M. *Organometallics* **1993**, *12*, 1714–1719.

(22) Smith, G. D.; Hanson, B. E.; Merola, J. S.; Waller, F. J. *Organometallics* **1993**, *12*, 568–570.

(23) Simpson, R. D.; Bergman, R. G. *Organometallics* **1993**, *12*, 781–96.

(24) Aldridge, T. K.; Stacy, E. M.; MacMillin, D. R. *Inorg. Chem.* **1994**, *33*, 722–727.

(25) Tóth, I.; Elsevier, C. J. *J. Chem. Soc., Chem. Commun.* **1993**, 529531.

(26) Woerpel, K. A.; Bergman, R. G. *J. Am. Chem. Soc.* **1993**, *115*, 7884.

(27) Osakada, K.; Ohshiro, K.; Yamamoto, A. *Organometallics* **1991**, *10*, 404–10.

(28) Churchill, M. R.; Fetting, J. C.; Rees, W. M.; Atwood, J. D. *J. Organomet. Chem.* **1986**, *304*, 361.

(29) Hayashi, Y.; Yamamoto, T.; Yamamoto, A.; Komiya, S.; Kushi, Y. *J. Am. Chem. Soc.* **1986**, *108*, 385–391.

(30) Cowan, R. L.; Trogler, W. C. *J. Am. Chem. Soc.* **1989**, *111*, 4750–61.

(31) Bugno, C. D.; Pasquali, M.; Leoni, P.; Sabatton, P.; Braga, D. *Inorg. Chem.* **1989**, *28*, 1390–1394.

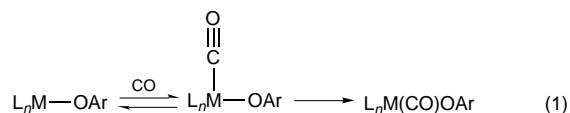
(32) Ni, J.; Kubiak, C. P. In *Homogeneous Transition Metal Catalyzed Reactions*; Moser, W. R., Slocum, D. W., Eds.; Advances in Chemistry Series; American Chemical Society: Washington, D C, 1992; Vol. 230, pp 515–528.

(33) Rees, W. M.; Churchill, M. R.; Fetting, J. C.; Atwood, J. D. *Organometallics* **1985**, *4*, 2179–2185.

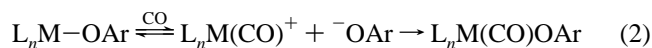
(34) Seligson, A. L.; Cowan, R. L.; Trogler, W. C. *Inorg. Chem.* **1991**, *30*, 3371–81.

energies in alkoxy complexes are comparable to the Pt–C ( $sp^3$ ) bond energies of the alkyl complexes.<sup>4</sup> Compared to the alkoxy complexes, the chemistry of late transition metal aryloxy complexes is expected to reflect a weaker M–O bond, inasmuch as the homolytic and heterolytic bond strengths for aryloxide complexes are expected to be lower.

There are two principal mechanisms by which late transition metal aryloxy complexes can be carbonylated to their respective (aryloxy)carbonyls. The first is classical migratory insertion,<sup>37</sup> where the aryloxy ligand migrates to a carbon monoxide *cis* to the aryloxy ligand, eq 1. Bryndza concluded that this mecha-



nism is important in the carbonylation of the platinum alkoxy complexes Pt(dppe)(OMe)(R) (R = OMe, Me; dppe = 1,2-bis-(diphenylphosphino)ethane).<sup>38</sup> This conclusion was based on NMR evidence of a five-coordinate carbon monoxide adduct, insertion rates that are faster than methoxide dissociation, and crossover studies that show no incorporation of labeled methoxide. A second type of mechanism that must be considered in view of the lower M–OAr bond energies expected for late transition metal aryloxy complexes is nucleophilic addition of the aryloxide to coordinated carbon monoxide. This involves substitution of a weakly bound aryloxy ligand by carbon monoxide, followed by nucleophilic addition of the displaced aryloxide to the carbonyl ligand, eq 2. Atwood *et al.* found



that nucleophilic addition of aryloxide to the coordinated carbon monoxide ligands of  $[Ir(CO)_2(PPh_3)_2]^+$  occurs during the reaction of  $Ir(CO)(PPh_3)_2(OR)$  (R = Me, Ph) with carbon monoxide.<sup>33</sup> Spectroscopic observation of the  $Ir(CO)_3(PPh_3)_2^+$  intermediate in quantities dependent on phenoxide basicity supported this conclusion.

We describe the synthesis of a series of new platinum aryloxy complexes and their reactions with carbon monoxide to give (aryloxy)carbonyl complexes. We present evidence, based on kinetic studies of the carbonylation reactions, concerning the mechanism of formation of the (aryloxy)carbonyl complexes.

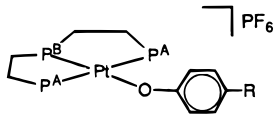
## Experimental Section

**General Considerations.**  $K_2PtCl_4$  was purchased from Aldrich Chemical Co. or obtained on loan from Johnson-Matthey. Triphos was purchased from Strem Chemical Co. Carbon monoxide (research grade) was purchased from Matheson. All phenols and sodium hydride were purchased from Aldrich. These materials were used without further purification. Sodium hexafluorophosphate was purchased from Aldrich, dried under vacuum at 150 °C for 36 h, and stored in an inert atmosphere glovebox.

Acetonitrile and methylene chloride were freshly distilled from  $CaH_2$  under a nitrogen atmosphere. Anhydrous *n*-heptane was purchased from Aldrich. Deuterated acetonitrile (99.9%) was purchased from Cambridge Isotope Labs. Deuterated acetonitrile and methylene chloride were stored under nitrogen and used as received.

<sup>1</sup>H and <sup>31</sup>P NMR spectra were recorded on a Varian XL-200 or General Electric QE-300 spectrometer. <sup>1</sup>H NMR spectra were refer-

**Table 1.** <sup>31</sup>P{<sup>1</sup>H} NMR Data for Complexes **2a–e**, [Pt(triphos)(OC<sub>6</sub>H<sub>4</sub>-*p*-R)][PF<sub>6</sub>]



R (compound)	P <sub>B</sub> , <i>trans</i> -phosphine <sup>c</sup>		P <sub>A</sub> , <i>trans</i> -phosphine <sup>c</sup>		Hammett $\sigma^b$
	$\delta(P_B)$ (ppm) <sup>a</sup>	<sup>1</sup> J(Pt–P <sub>B</sub> ) (Hz)	$\delta(P_A)$ (ppm) <sup>a</sup>	<sup>1</sup> J(Pt–P <sub>A</sub> ) (Hz)	
Cl ( <b>2e</b> )	75.69	2870.4	40.89	2608.8	0.23
F ( <b>2d</b> )	75.48	2840.9	40.80	2633.8	0.06
H ( <b>2c</b> )	75.53	2835.4	40.32	2620.0	0.00
Me ( <b>2b</b> )	75.26	2808.8	40.31	2641.2	–0.17
OMe ( <b>2a</b> )	75.09	2795.4	40.40	2649.5	–0.27

<sup>a</sup> Recorded at 80.98 MHz in CD<sub>3</sub>CN at 293 K; chemical shifts are relative to external 85% H<sub>3</sub>PO<sub>4</sub> at 0.00 ppm. <sup>b</sup> The Hammett  $\sigma$ -values<sup>47</sup> are included as a reference to the electron-donating nature of the aryloxide. <sup>c</sup> The <sup>2</sup>J(P<sub>A</sub>–P<sub>B</sub>) coupling constant for **2a–e** is 3 Hz.

enced to external TMS via residual solvent peaks. <sup>31</sup>P NMR spectra were referenced to external 85% H<sub>3</sub>PO<sub>4</sub> and were all proton decoupled. Infrared spectra were obtained using a Perkin-Elmer 1710 Fourier transform spectrometer with a 1700/PC data station.

All reactions and manipulations were carried out under a nitrogen atmosphere using a nitrogen-filled glovebox (Vacuum Atmospheres) or by standard Schlenk line techniques. The NaOC<sub>6</sub>H<sub>4</sub>R reagents were prepared from the corresponding phenol and a 5-fold excess of NaH in THF. Unreacted NaH was filtered off, the filtrate concentrated, and hexane added to precipitate the white product. Pt(cod)Cl<sub>2</sub> (cod = 1,5-cyclooctadiene) was prepared by a published literature procedure.<sup>39</sup>

**Synthesis of [Pt(triphos)(Cl)][Cl] (**1**).** This complex was prepared by modification of the previously reported synthesis of Pt(dmpe)Cl<sub>2</sub> (dmpe = 1,2-bis(dimethylphosphino)ethane).<sup>40,41</sup> A solution of Pt(cod)Cl<sub>2</sub> (1.63 g, 4.33 mmol) in methylene chloride (30 mL) was added to a solution of triphos (2.32 g, 4.33 mmol) in methylene chloride (30 mL). After 30 min, the solvent was removed *in vacuo* to give a white solid which was washed with diethyl ether and recrystallized from methylene chloride/heptane. Compound **1** was isolated as a white solid and dried under vacuum. Yield: 2.84 g, 81.4%. <sup>1</sup>H NMR (CD<sub>2</sub>Cl<sub>2</sub>, 300 MHz,  $\delta$ , ppm): 2.2 (m, 2H, P-CH<sub>2</sub>), 2.7 (m, 2H, P-CH<sub>2</sub>), 3.1 (m, 2H, P-CH<sub>2</sub>), 3.8 (m, 2H, P-CH<sub>2</sub>), 7.5–8.4 (m, 25H, triphos phenyl). <sup>31</sup>P{<sup>1</sup>H} NMR (CD<sub>3</sub>CN, 80.98 MHz,  $\delta$ , ppm): A<sub>2</sub>BX, (P<sub>A</sub>) 42.27, <sup>1</sup>J(P<sub>A</sub>–Pt) = 2483.6 Hz; (P<sub>B</sub>) 86.34, <sup>1</sup>J(P<sub>B</sub>–Pt) = 3027.8 Hz, <sup>2</sup>J(P<sub>A</sub>–P<sub>B</sub>) = 1.5 Hz.

**Preparation of Aryloxide Complexes.** <sup>31</sup>P{<sup>1</sup>H} NMR for complexes **2a–e** are presented in Table 1. The designation P<sub>A</sub> refers to phosphorus nuclei *cis* to the aryloxide, and P<sub>B</sub> refers to the phosphorus nucleus *trans* to the aryloxide.

**Synthesis of [Pt(triphos)(OC<sub>6</sub>H<sub>4</sub>-*p*-OMe)][PF<sub>6</sub>] (**2a**).** To an acetonitrile (7 mL) solution of NaPF<sub>6</sub> (0.1898 g, 1.1300 mmol) and [Pt(triphos)(Cl)][Cl] (0.2459 g, 0.3072 mmol) was added NaOC<sub>6</sub>H<sub>4</sub>-*p*-Me (0.0523 g, 0.3233 mmol), giving a light yellow solution. After 10 min the solvent was removed *in vacuo*. The remaining solid was redissolved in methylene chloride, the solution filtered, and the filtrate dried *in vacuo* to give a yellow solid. Yield: 0.2645 g, 85.0%. <sup>1</sup>H NMR (CD<sub>3</sub>CN, 200 MHz,  $\delta$ , ppm): 3.4 (s, 3H, OCH<sub>3</sub>), 2.1–3.3 (m, 8H, P-CH<sub>2</sub>), 6.2 (d, 2H, CH), 6.4 (d, 2H, CH), 7.2–8.2 (m, 25H, triphos phenyl). Anal. Calcd for C<sub>41</sub>H<sub>40</sub>O<sub>2</sub>F<sub>6</sub>P<sub>4</sub>Pt: C, 49.96; H, 3.99. Found: C, 49.02; H, 3.94.

**Synthesis of [Pt(triphos)(OC<sub>6</sub>H<sub>4</sub>-*p*-Me)][PF<sub>6</sub>] (**2b**).** This complex was prepared similarly to **2a** from NaPF<sub>6</sub> (0.1137 g, 0.6770 mmol), [Pt(triphos)(Cl)][Cl] (0.1924 g, 0.2405 mmol), and NaOC<sub>6</sub>H<sub>4</sub>-*p*-Me

(35) Hartwig, J. F.; Andersen, R. A.; Bergman, R. G. *Organometallics* **1991**, *10*, 1875–87.

(36) Ladipo, F. T.; Kooti, M.; Merola, J. S. *Inorg. Chem.* **1993**, *32*, 1681–1688.

(37) Flood, T. C.; Jensen, J. E.; Statler, J. A. *J. Am. Chem. Soc.* **1981**, *103*, 4410–14.

(38) Bryndza, H. E. *Organometallics* **1985**, *4*, 1686–7.

(39) McDermott, J. X.; White, J. F.; Whitesides, G. M. *J. Am. Chem. Soc.* **1976**, *98*, 6521–6528.

(40) Anderson, G. K.; Lumetta, G. J. *Inorg. Chem.* **1987**, *26*, 1518–1524.

(41) Although first prepared in 1971 by King *et al.* (*Inorg. Chem.* **1971**, *10*, 1841–50), this synthesis requires less time. The yields are similar to the earlier preparation and give a product spectroscopically identical to that reported for [Pt(triphos)(Cl)][Cl].

**Table 2.**  $^{31}\text{P}\{^1\text{H}\}$  NMR Data for Complexes **3a–c**,  $[\text{Pt}(\text{triphos})(\text{C}(\text{O})\text{OC}_6\text{H}_4\text{-}p\text{-R})][\text{PF}_6]$ 

R (compound)	$\text{P}_\text{B}$ , <i>trans</i> -phosphine <sup>c</sup>		$\text{P}_\text{A}$ , <i>cis</i> phosphine <sup>c</sup>		Hammett $\sigma^b$
	$\delta(\text{P}_\text{B})$ (ppm) <sup>a</sup>	$^1J(\text{Pt}-\text{P}_\text{B})$ (Hz)	$\delta(\text{P}_\text{A})$ (ppm) <sup>a</sup>	$^1J(\text{Pt}-\text{P}_\text{A})$ (Hz)	
Cl ( <b>3e</b> )	90.86	1665.8	40.04	2607.6	0.23
F ( <b>3d</b> )	90.88	1658.5	40.01	2611.1	0.06
H ( <b>3c</b> )	90.79	1648.0	39.75	2622.3	0.00
Me ( <b>3b</b> )	90.71	1642.4	39.70	2627.9	-0.17
OMe ( <b>3a</b> )	90.55	1643.1	39.60	2626.4	-0.27

<sup>a</sup> Recorded at 80.98 MHz in  $\text{CD}_3\text{CN}$  at 293 K; chemical shifts are relative to external 85%  $\text{H}_3\text{PO}_4$  at 0.00 ppm. <sup>b</sup> The Hammett  $\sigma$  values<sup>47</sup> are included as a reference to the electron-donating nature of the aryloxy. <sup>c</sup> The  $^2J(\text{P}_\text{A}-\text{P}_\text{B})$  coupling constant for **3a–e** is 6 Hz.

(0.0369 g, 0.2532 mmol) and was isolated as a yellow solid. Yield: 0.2100 g, 89.0%.  $^1\text{H}$  NMR ( $\text{CD}_3\text{CN}$ , 300 MHz,  $\delta$ , ppm): 2.1 (s, 3H,  $\text{PhCH}_3$ ), 2.2–3.6 (m, 8H,  $\text{P-CH}_2$ ), 6.5 (d, 2H,  $\text{CH}$ ), 6.8 (d, 2H,  $\text{CH}$ ), 7.2–8.2 (m, 25H, triphos phenyl). Anal. Calcd for  $\text{C}_{41}\text{H}_{40}\text{OF}_6\text{P}_4\text{Pt}$ : C, 50.16; H, 4.11. Found: C, 50.04; H, 4.48.

**Synthesis of  $[\text{Pt}(\text{triphos})(\text{OPh})][\text{PF}_6]$  (**2c**).** This complex was prepared similarly to **2a** from  $\text{NaPF}_6$  (0.1049 g, 0.6249 mmol),  $[\text{Pt}(\text{triphos})(\text{Cl})][\text{Cl}]$  (0.1667 g, 0.2082 mmol), and  $\text{NaOPh}$  (0.0248 g, 0.2193 mmol) and was isolated as a light yellow solid. Yield: 0.1730 g, 86.1%.  $^1\text{H}$  NMR ( $\text{CD}_3\text{CN}$ , 300 MHz,  $\delta$ , ppm): 2.1–3.4 (m, 8H,  $\text{P-CH}_2$ ), 6.5 (m, 3H,  $\text{CH}$ ), 7.0 (d, 2H,  $\text{CH}$ ), 7.2–8.2 (m, 25H, triphos phenyl). Anal. Calcd for  $\text{C}_{40}\text{H}_{38}\text{OF}_6\text{P}_4\text{Pt}$ : C, 49.65; H, 3.96. Found: C, 49.69; H, 4.12.

**Synthesis of  $[\text{Pt}(\text{triphos})(\text{OC}_6\text{H}_4\text{-}p\text{-F})][\text{PF}_6]$  (**2d**).** This complex was prepared similarly to **2a** from  $\text{NaPF}_6$  (0.4245 g, 2.5275 mmol),  $[\text{Pt}(\text{triphos})(\text{Cl})][\text{Cl}]$  (0.4394, 0.5488 mmol), and  $\text{NaOC}_6\text{H}_4\text{-}p\text{-F}$  (0.1089 g, 0.8122 mmol) and was isolated as a light yellow solid. Yield: 0.5146 g, 95.1%.  $^1\text{H}$  NMR ( $\text{CD}_3\text{CN}$ , 300 MHz,  $\delta$ , ppm): 2.1–3.4 (m, 8H,  $\text{P-CH}_2$ ), 6.3 (m, 2H,  $\text{CH}$ ), 6.3 (m, 2H,  $\text{CH}$ ), 7.2–8.1 (m, 25H, triphos phenyl). Anal. Calcd for  $\text{C}_{40}\text{H}_{37}\text{OF}_7\text{P}_4\text{Pt} \cdot \frac{1}{2}\text{CH}_2\text{Cl}_2$ : C, 47.31; H, 3.73. Found: C, 47.71; H, 3.71.<sup>42</sup>

**Synthesis of  $[\text{Pt}(\text{triphos})(\text{OC}_6\text{H}_4\text{-}p\text{-Cl})][\text{PF}_6]$  (**2e**).** This complex was prepared similarly to **2a** from  $\text{NaPF}_6$  (0.24 g, 1.43 mmol),  $[\text{Pt}(\text{triphos})(\text{Cl})][\text{Cl}]$  (0.1601 g, 0.2000 mmol), and  $\text{NaOC}_6\text{H}_4\text{-}p\text{-Cl}$  (0.0602 g, 0.3999 mmol) and was isolated as a light yellow solid. Yield: 0.1740 g, 87.0%.  $^1\text{H}$  NMR ( $\text{CD}_3\text{CN}$ , 300 MHz,  $\delta$ , ppm): 2.1–3.5 (m, 8H,  $\text{P-CH}_2$ ), 6.4 (d, 2H,  $\text{CH}$ ), 6.5 (d, 2H,  $\text{CH}$ ), 7.3–8.1 (m, 25H, triphos phenyl). Anal. Calcd for  $\text{C}_{40}\text{H}_{37}\text{OClF}_6\text{P}_4\text{Pt}$ : C, 47.94; H, 3.72. Found: C, 47.75; H, 3.73.

**Preparation of (Aryloxy)carbonyl Complexes.**  $^{31}\text{P}\{^1\text{H}\}$  NMR for complexes **3a–e** in acetonitrile- $d_3$  were recorded *in situ* using high-pressure NMR tubes pressurized with carbon monoxide. Results are presented in Table 2. The designation where  $\text{P}_\text{A}$  refers to phosphorus nuclei *cis* to the (aryloxy)carbonyl and  $\text{P}_\text{B}$  refers to phosphorus nucleus *trans* to the (aryloxy)carbonyl is retained.

**Synthesis of  $[\text{Pt}(\text{triphos})(\text{C}(\text{O})\text{OC}_6\text{H}_4\text{-}p\text{-OMe})][\text{PF}_6]$  (**3a**).** A pressure valve NMR tube (Wilmad), containing a methylene chloride (1.5 mL) solution of  $[\text{Pt}(\text{triphos})(\text{OC}_6\text{H}_4\text{-}p\text{-OMe})][\text{PF}_6]$  (**2a**) (0.0319 g, 0.0315 mmol), was carefully layered with heptane and pressurized with 100 psi (gauge pressure) of carbon monoxide. The tube was allowed to stand for 3 days at room temperature until yellow crystals formed. IR (KBr):  $\nu(\text{CO}) = 1655 \text{ cm}^{-1}$ . Anal. Calcd for  $\text{C}_{42}\text{H}_{40}\text{O}_3\text{F}_6\text{P}_4\text{Pt}$ : C, 49.18; H, 3.93. Found: C, 49.17; H, 3.95.

**Synthesis of  $[\text{Pt}(\text{triphos})(\text{C}(\text{O})\text{OC}_6\text{H}_4\text{-}p\text{-Me})][\text{PF}_6]$  (**3b**).** This complex was prepared similarly to **3a** from a methylene chloride (1.5 mL) solution containing  $[\text{Pt}(\text{triphos})(\text{OC}_6\text{H}_4\text{-}p\text{-Me})][\text{PF}_6]$  (**2b**) (0.1326 g, 0.1351 mmol). Yield: 0.0623 g, 45.7%. IR (KBr):  $\nu(\text{CO}) = 1677 \text{ cm}^{-1}$ . Anal. Calcd for  $\text{C}_{42}\text{H}_{40}\text{O}_2\text{F}_6\text{P}_4\text{Pt}$ : C, 49.96; H, 3.99. Found: C, 49.35; H, 4.01.

**Reaction of  $[\text{Pt}(\text{triphos})(\text{OPh})][\text{PF}_6]$  (**2c**) with Carbon Monoxide.** The complex  $[\text{Pt}(\text{triphos})(\text{C}(\text{O})\text{OPh})][\text{PF}_6]$  (**3c**) was prepared *in situ* from a methylene chloride (1.5 mL) solution containing  $[\text{Pt}(\text{triphos})(\text{OPh})][\text{PF}_6]$  (**2c**) (0.0450 g, 0.0466 mmol) pressurized with 100 psi

(gauge pressure) of carbon monoxide. Although the reaction proceeds to completion, the product from this NMR scale reaction was not isolated.

**Synthesis of  $[\text{Pt}(\text{triphos})(\text{C}(\text{O})\text{OC}_6\text{H}_4\text{-}p\text{-F})][\text{PF}_6]$  (**3d**).** This complex was prepared similarly to **3a** from a methylene chloride (1.5 mL) solution containing  $[\text{Pt}(\text{triphos})(\text{OC}_6\text{H}_4\text{-}p\text{-F})][\text{PF}_6]$  (**2d**) (0.0151 g, 0.0153 mmol). Yield: 0.0076 g, 48.0%. IR (KBr):  $\nu(\text{CO}) = 1673 \text{ cm}^{-1}$ .

**Reaction of  $[\text{Pt}(\text{triphos})(\text{OC}_6\text{H}_4\text{-}p\text{-Cl})][\text{PF}_6]$  (**2e**) with Carbon Monoxide.** The complex  $[\text{Pt}(\text{triphos})(\text{C}(\text{O})\text{OC}_6\text{H}_4\text{-}p\text{-Cl})][\text{PF}_6]$  (**3e**) was prepared *in situ* from a methylene chloride (1.5 mL) solution containing  $[\text{Pt}(\text{triphos})(\text{OC}_6\text{H}_4\text{-}p\text{-Cl})][\text{PF}_6]$  (**2e**) (0.0450 g, 0.0466 mmol) pressurized with carbon monoxide. This reaction was found by  $^{31}\text{P}\{^1\text{H}\}$  NMR to proceed only to 90% completion with 100 psi (gauge pressure) of carbon monoxide, and the complex was not isolated.

**Collection of X-ray Diffraction Data for  $[\text{Pt}(\text{triphos})(\text{C}(\text{O})\text{OC}_6\text{H}_4\text{-}p\text{-Me})][\text{PF}_6]$  (**3b**).** Crystals suitable for a single-crystal X-ray diffraction study were grown by placing a methylene chloride solution of  $[\text{Pt}(\text{triphos})(\text{OC}_6\text{H}_4\text{-}p\text{-Me})][\text{PF}_6]$  (**2b**) into a pressure valve NMR tube. The solution was then carefully layered with dry heptane, and 100 psi of carbon monoxide was introduced into the tube. A pale yellow crystal of  $\text{C}_{42}\text{H}_{40}\text{PtF}_6\text{O}_2\text{P}_4$  having approximate dimensions of  $0.35 \times 0.28 \times 0.24 \text{ mm}$  was mounted on a glass fiber in a random orientation. The structure was solved using the Patterson method which revealed the position of the Pt atom. The remaining atoms were located in succeeding difference Fourier syntheses. Hydrogen atoms were located and added to the structure factor calculations, but their positions were not refined. The final cycle of refinement converged with  $R = 0.035$  and  $R_w = 0.040$ . Plots of  $\sum_w(|F_o| - |F_c|)^2$  versus  $|F_o|$ , reflection order in data collection,  $\sin \theta/\lambda$ , and various classes of indices showed no unusual trends. The highest peak in the final difference Fourier had a height of  $0.67 \text{ e}/\text{\AA}^3$ . The crystallographic data are summarized in Table 3. An ORTEP drawing of **3b** is presented in Figure 1. Selected bond distances and angles are listed in Table 4.

**Kinetic Studies.** Rates of carbonylation of **2a–d** were followed by  $^{31}\text{P}\{^1\text{H}\}$  NMR under carbon monoxide pressure at ambient temperatures.<sup>43</sup> In a typical experiment, a pressure NMR tube (Wilmad) was charged in an inert atmosphere box with an acetonitrile- $d_3$  solution of one of the platinum aryloxy complexes **2a–d**. Experiments with excess aryloxy ligand required a 1:1 acetonitrile- $d_3$ /THF solvent mixture. An initial  $^{31}\text{P}\{^1\text{H}\}$  NMR spectrum was taken before the tube was evacuated and pressurized (10–134 psi gauge) with carbon monoxide.  $^{31}\text{P}\{^1\text{H}\}$  NMR spectra were then taken at regular intervals. Signals corresponding to the starting aryloxy complexes **2a–d** and the carbonylated (aryloxy)carbonyl product, **3a–d** were integrated, and these integrations were used in the kinetic data analysis. Spin–lattice relaxation times ( $T_1$ ) for **2a** were determined by inversion recovery for  $\text{P}_\text{A}$  (4.8 s) and  $\text{P}_\text{B}$  (3.4 s). To obtain accurate integrations, a single  $35^\circ$  pulse was used with a 6 s recycle rate and a 2 s acquisition time. The pressure NMR tubes were individually calibrated so that sample volumes could be easily determined from sample height. The total volume of the tubes was also calibrated. The concentration of carbon monoxide in acetonitrile was determined by Henry's law.<sup>44</sup>

## Results and Discussion

**Synthesis of Platinum Aryloxy Complexes.** The synthesis of the platinum aryloxy complexes  $[\text{Pt}(\text{triphos})(\text{OC}_6\text{H}_4\text{-}p\text{-R})][\text{PF}_6]$  **2a–e** proceeds by a metathesis reaction involving  $[\text{Pt}(\text{triphos})(\text{Cl})][\text{Cl}]$  and  $\text{NaOC}_6\text{H}_4\text{-}p\text{-R}$ , eq 3. The anion exchange is done concurrently by performing the reaction in the presence of excess  $\text{NaPF}_6$ .  $^{31}\text{P}\{^1\text{H}\}$  NMR provides an excellent means of characterizing platinum triphos complexes. The very small

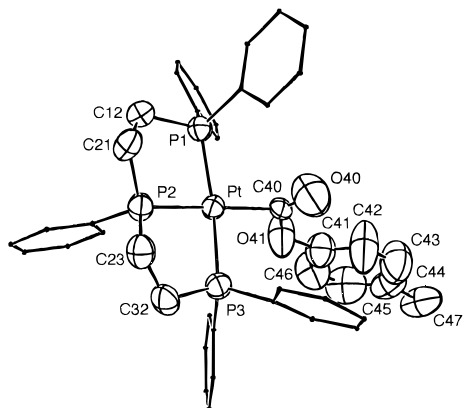
(43) Ambient room temperature in the NMR probe is ca.  $22^\circ\text{C}$ . During the reaction the NMR tube was not removed from the probe. Due to probe design, the probe cooling air provides a thermostatic environment. Experiments with the NMR chemical shift thermometer have shown that the probe temperature would vary by less than  $\pm 1^\circ\text{C}$  over the length of the experiment. Sample heating during the actual NMR experiment, due to decoupling, should be minimal as low power WALTZ decoupling was used.

(44) Fogg, P. G. T.; Gerrard, W. *Solubility of Gases in Liquids, A Critical Evaluation of Gas/Liquid Systems in Theory and Practice*; John Wiley and Sons: New York, 1991.

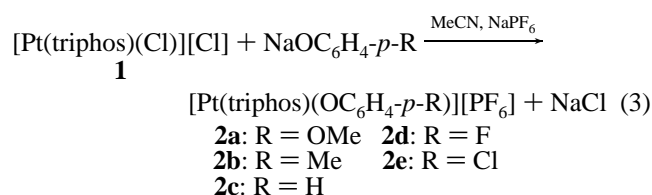
(42) Solvent incorporation verified by  $^1\text{H}$  NMR.

**Table 3.** Structure Determination Summary for [Pt(triphos)C(O)OC<sub>6</sub>H<sub>4</sub>-*p*-Me][PF<sub>6</sub>] (**3b**)

formula	PtP <sub>3</sub> F <sub>6</sub> O <sub>2</sub> C <sub>42</sub> H <sub>40</sub>	crystal dimensions, mm	0.35 × 0.28 × 0.24
formula weight	1009.76	temperature, K	293
crystal system	monoclinic	radiation (wavelength)	Mo Kα (0.710 73 Å)
space group	<i>P</i> 2 <sub>1</sub> / <i>n</i> (no. 14)	$\mu$ , cm <sup>-1</sup>	36.97
<i>a</i> , Å	10.797(1)	<i>h</i> , <i>k</i> , <i>l</i> range	−12 to +12, −22 to 0, 0 to 21
<i>b</i> , Å	19.927(3)	no. of data collected	6839
<i>c</i> , Å	19.113(2)	no. of unique data	6626
$\beta$ , deg	98.07(1)	no. of data with <i>I</i> > 3.0σ( <i>I</i> )	3958
<i>V</i> , Å <sup>3</sup>	4071(2)	no. of variables	496
<i>Z</i>	4	<i>R</i>	0.035
<i>d</i> <sub>calc</sub> , g cm <sup>-3</sup>	1.647	<i>R</i> <sub>w</sub>	0.040

**Figure 1.** ORTEP drawing of [Pt(triphos)C(O)OC<sub>6</sub>H<sub>4</sub>Me][PF<sub>6</sub>] (**3b**) showing 50% probability ellipsoids and the atomic labeling. Hydrogen atoms are not shown, and ligand phenyl carbons are shown as points for clarity.**Table 4.** Selected Bond Distances (Å) and Torsion and Bond Angles (deg) for [Pt(triphos)C(O)OC<sub>6</sub>H<sub>4</sub>-*p*-Me][PF<sub>6</sub>] (**3b**)

Bond Distances			
Pt–P(1)	2.296(2)	O(41)–C(40)	1.28(1)
Pt–P(2)	2.254(2)	O(41)–C(41)	1.44(1)
Pt–P(3)	2.292(2)	C(41)–C(42)	1.38(2)
Pt–C(40)	2.111(8)	C(41)–C(46)	1.36(1)
O(40)–C(40)	1.08(1)		
Bond and Torsion Angles			
P(1)–Pt–P(2)	85.38(8)	Pt–C(40)–O(40)	122.1(7)
P(1)–Pt–P(3)	168.60(8)	Pt–C(40)–O(41)	110.2(6)
P(1)–Pt–C(40)	96.5(2)	O(40)–C(40)–O(41)	126.0(8)
P(2)–Pt–P(3)	85.03(8)	O(41)–C(41)–C(42)	124.1(1)
P(2)–Pt–C(40)	174.9(2)	O(41)–C(41)–C(46)	115.6(9)
P(3)–Pt–C(40)	92.5(2)	P(1)–Pt–C(40)–O(40)	75.4(9)
C(40)–O(41)–C(41)	125.7(8)	P(1)–Pt–C(40)–O(41)	118.6(6)



<sup>2</sup>*J*(P<sub>A</sub>–P<sub>B</sub>) couplings are consistent with the expected square planar structure of these complexes.<sup>45</sup> Furthermore, the <sup>1</sup>*J*(P<sub>B</sub>–Pt) coupling constants are sensitive to the nature of the ligand *trans* to P<sub>B</sub>.<sup>46</sup> For example, as the electron-withdrawing nature of the *para*-substituent on the arene ring of the aryloxy ligands is increased from R = OMe (**2a**) to R = Cl (**2e**), <sup>1</sup>*J*(P<sub>B</sub>–Pt) systematically increases from 2795 to 2870 Hz; <sup>31</sup>P{<sup>1</sup>H} NMR data for **2a–e** are summarized in Table 1. The trend evident in the <sup>31</sup>P{<sup>1</sup>H} NMR data is rationalized by a “push-pull” *trans*

influence in which the increased electron-withdrawing nature of the *para*-substituent leads to increases in <sup>1</sup>*J*(P<sub>B</sub>–Pt) coupling constants. The increasing P<sub>B</sub>–Pt interaction occurs in response to the presence of progressively weaker Pt–O(C<sub>6</sub>H<sub>4</sub>-*p*-R) bonds, *trans* to P<sub>B</sub>, as the electron-withdrawing nature of the *para* substituent is increased. This effect of the *para*-substituents on the <sup>1</sup>*J*(P<sub>B</sub>–Pt) coupling constants correlates with Hammett  $\sigma$ -values.<sup>47</sup> This correlation gives a best fit equation of <sup>1</sup>*J*(P<sub>B</sub>–Pt) = (149.3 Hz)σ + 2834.61; *R*<sup>2</sup> = 0.997. The slope of this correlation, 149.3 Hz, is not a conventional Hammett  $\delta$ , which refers to the susceptibility of a reaction's rate to electronic effects. However, correlation of NMR parameters with Hammett  $\sigma$  provides a useful framework for comparison. Furthermore, correlations between Hammett  $\sigma$  and <sup>1</sup>H NMR parameters of substituted phenols<sup>48</sup> and arylcarbinols<sup>49,50</sup> are reported in the literature.

**Carbonylation Reactions.** When [Pt(triphos)(OC<sub>6</sub>H<sub>4</sub>-*p*-R)]-[PF<sub>6</sub>] is reacted with as little as 10 psi of carbon monoxide, the <sup>31</sup>P{<sup>1</sup>H} NMR shows a downfield shift of the phosphorus atom *trans* to the aryloxy, P<sub>B</sub>, along with a decrease in the <sup>1</sup>*J*(Pt–P<sub>B</sub>) coupling constant. These changes are characteristic of carbon monoxide insertion.<sup>14,32,38</sup> The replacement of the sp<sup>3</sup> oxygen with an sp<sup>2</sup> carbon puts a ligand with more  $\sigma$ -character, and larger *trans* influence, opposite P<sub>B</sub>. The increased  $\sigma$ -donation from the (aryloxy)carbonyl ligand is reflected in a smaller <sup>1</sup>*J*(Pt–P<sub>B</sub>) coupling constant, for the phosphorus *trans* to the (aryloxy)carbonyl. For example, when carbon monoxide inserts into the Pt–O bond of [Pt(triphos)(OC<sub>6</sub>H<sub>4</sub>-*p*-Me)][PF<sub>6</sub>], the <sup>1</sup>*J*(Pt–P<sub>B</sub>) coupling constant decreases from 2808.8 to 1642.4 Hz, and the chemical shift of P<sub>B</sub> moves downfield from 75.3 to 90.7 ppm. The <sup>31</sup>P{<sup>1</sup>H} NMR data for the carbonylated products **3a–e** are summarized in Table 2. For the phosphorus atoms *cis* to the (aryloxy)carbonyl, the small observed changes in chemical shift and <sup>1</sup>*J*(Pt–P<sub>A</sub>) values can be interpreted in terms of only minor overall structural changes occurring upon reaction with carbon monoxide. When the carbonylation is followed by <sup>31</sup>P{<sup>1</sup>H} NMR, starting material is seen to cleanly convert to product; no other products or intermediates are seen, Figure 2. The IR spectra of compounds **3a,b,d** show (aryloxy)carbonyl  $\nu$ (CO) bands at 1677, 1655, and 1673 cm<sup>-1</sup>, respectively, consistent with published spectra of other alkoxy-carbonyls.<sup>14,33,38</sup>

**Crystal and Molecular Structure of [Pt(triphos)(C(O)-OC<sub>6</sub>H<sub>4</sub>-*p*-Me)][PF<sub>6</sub>] (**3b**).** The crystal and molecular structure of the [(*p*-methylaryl)oxy]carbonyl complex **3b** was determined. This is the first X-ray structure determination of an (aryloxy)-carbonyl complex. Selected bond distances and angles are summarized in Table 3. An ORTEP drawing of the molecular cation [Pt(triphos)(C(O)OC<sub>6</sub>H<sub>4</sub>-*p*-Me)]<sup>+</sup> is given in Figure 1.

(47) McDaniel, D. H.; Brown, H. C. *J. Org. Chem.* **1958**, 23, 420.(48) Ouellette, R. J. *Can. J. Chem.* **1965**, 43, 707–709.(49) Bobko, E.; Tolerico, C. S. *J. Org. Chem.* **1983**, 48, 1368–1369.(50) Ouellette, R. J.; Marks, D. L.; Miller, D. *J. Am. Chem. Soc.* **1967**, 89, 913–917.(45) Karplus, M. *J. Chem. Phys.* **1959**, 30, 11.(46) Hartley, F. R. *The Chemistry of Platinum and Palladium*; Halsted Press: New York, 1973; p 303.

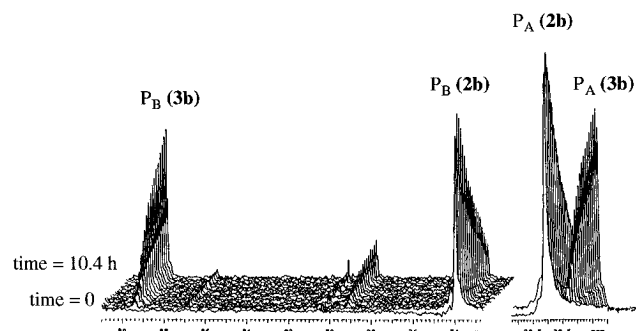


**Figure 2.** Overlaid  $^{31}\text{P}\{^1\text{H}\}$  spectra showing the disappearance of resonances corresponding to the aryloxy **2b** and the appearance of the (aryloxy)carbonyl **3b**.

The central  $d^8$  platinum(II) atom has a distorted square planar geometry; the two *trans* angles are  $\text{P}(1)\text{--Pt--P}(3) = 168.60(8)^\circ$  and  $\text{P}(2)\text{--Pt--C}(40) = 174.9(2)^\circ$ . Several differences are apparent between **3b** and the related, structurally characterized alkoxy-carbonyls: *trans*- $\text{Pt}(\text{C}(\text{O})\text{OEt})_2(\text{PPh}_3)_2$ ,<sup>8</sup>  $\text{Pt}(\text{C}(\text{O})\text{OMe})_2(\text{dppe})$ ,<sup>14</sup> *trans*- $\text{Pt}(\text{C}(\text{O})\text{OMe})(\text{C}(\text{O})\text{Ph})(\text{PPh}_3)_2$ ,<sup>6</sup> and  $\text{Pt}(\text{C}(\text{O})\text{OEt})(\text{C}\equiv\text{C}(\text{O})\text{OMe})(\text{PPh}_3)_2$ .<sup>7</sup> The most striking difference is the  $\text{C}(40)\text{--O}(40)$  bond distance of  $1.08(1) \text{ \AA}$ , similar in length to weakly back-bonded terminal carbonyls. It must be noted that the thermal ellipsoid of the carbonyl oxygen is distorted along the  $\text{C}(40)\text{--O}(40)$  bond axis, such that this bond length is artificially shortened. For the complex  $\text{Pt}(\text{dppe})(\text{C}(\text{O})\text{OMe})_2$ , Bryndza reports carbonyl bond distances of  $1.191$  and  $1.202 \text{ \AA}$ .<sup>14</sup> Alkoxy-carbonyl  $\text{C--O}$  bond distances in the range of  $1.191\text{--}1.228(7) \text{ \AA}$  are seen for all of the aforementioned complexes. The  $\text{C}(40)\text{--O}(41)$  bond distance of  $1.28(1) \text{ \AA}$  in **3b** is also approximately  $0.077(10) \text{ \AA}$  shorter than the average distance of  $1.357(9) \text{ \AA}$  seen for the related complexes. Interestingly the longest and shortest bond distances,  $1.372$  and  $1.350 \text{ \AA}$ , for this group are seen in  $\text{Pt}(\text{C}(\text{O})\text{OMe})_2(\text{dppe})$ .<sup>14</sup> The  $\text{Pt--C}(40)$  bond distance is  $2.111(9) \text{ \AA}$ , approximately  $0.1 \text{ \AA}$  longer than  $\text{Pt--C}$  distances reported for the related complexes. For the complex  $\text{Pt}(\text{dppe})(\text{C}(\text{O})\text{OMe})_2$  Bryndza reports the  $\text{Pt--C}$  bonds to be  $2.057$  and  $2.065 \text{ \AA}$ ,<sup>14</sup> while Sen reports the  $\text{Pt--C}$  bond as  $2.032(9) \text{ \AA}$  for  $\text{Pt}(\text{PPh}_3)_2(\text{C}(\text{O})\text{Ph})(\text{C}(\text{O})\text{OMe})$ .<sup>6</sup> The origin of these differences is probably not due to the presence of an aromatic ring, but rather it is more likely due to the cationic nature of complex **3b**. If the presence of an aromatic ring were a primary factor, one would expect some deviation in the aryl carbon--oxygen  $\text{O}(41)\text{--C}(41)$  bond length of  $1.44(1) \text{ \AA}$ . The  $\text{O}(41)\text{--C}(41)$  distance is comparable to the  $\text{C--O}$  bond length of  $1.401(10) \text{ \AA}$ , typical of aromatic esters.<sup>51</sup> The  $\text{C--O}$  bonds in *trans*- $\text{Pt}(\text{C}(\text{O})\text{OEt})_2(\text{PPh}_3)_2$ <sup>8</sup> and  $\text{Pt}(\text{C}(\text{O})\text{OEt})(\text{C}\equiv\text{C}(\text{O})\text{OMe})(\text{PPh}_3)_2$ <sup>7</sup> at  $1.459(11) \text{ \AA}$  and  $1.436(16) \text{ \AA}$  are also comparable. Apparently, the cationic nature of the platinum center in **3b** results in poorer orbital overlap and a longer  $\text{Pt--C}$  bond. The result is more electron density on the carbonyl carbon atom,  $\text{C}(40)$ , and shorter  $\text{C}(40)\text{--O}(40)$  and  $\text{C}(40)\text{--O}(41)$  bonds. A final structural point regarding **3b** is that the (aryloxy)carbonyl group adopts a geometry that is tilted  $75.4(9)^\circ$  with respect to the  $\text{PtP}_3\text{C}$  plane, while comparable alkoxy-carbonyls adopt a nearly perpendicular orientation.<sup>6,7,14,52</sup>

**Kinetics of Carbonylation.** The carbonylations of **2a--d** were followed by  $^{31}\text{P}\{^1\text{H}\}$  NMR at ambient temperatures, Figure 2. The kinetics of carbonylation are first order in **[2a--d]** to better than 4 half-lives. Varying the carbon monoxide pressures from 50 to 134 psi also indicated that the observed rates were

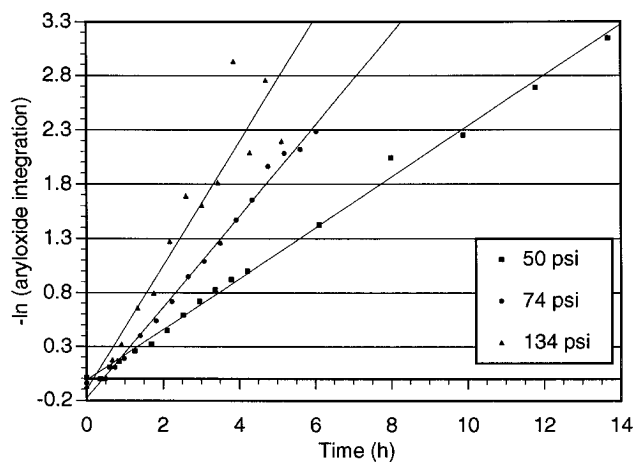


**Figure 3.** Dependence of the observed rate of  $[(p\text{-methylaryl})\text{oxy}]$ -carbonyl formation on carbon monoxide pressure for  $[\text{Pt}(\text{triphos})(\text{C}(\text{O})\text{OC}_6\text{H}_4\text{-}p\text{-Me})][\text{PF}_6]$  (**2b**).

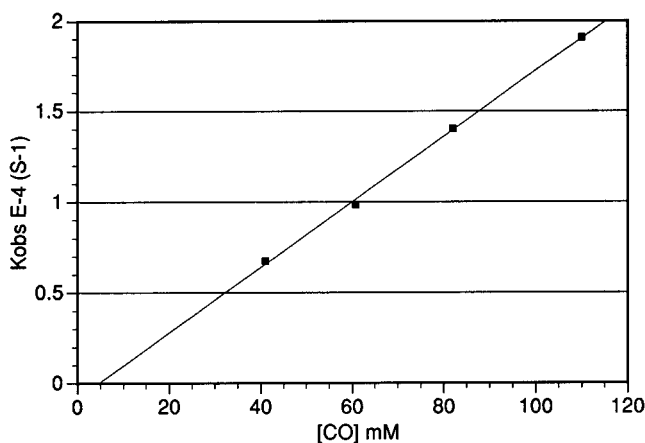
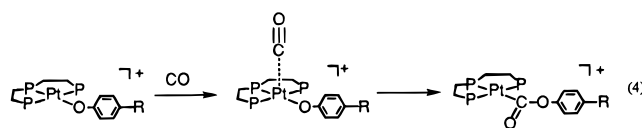


**Figure 4.** Change in the observed rate of  $[(p\text{-methylaryl})\text{oxy}]$ -carbonyl formation vs carbon monoxide concentration for  $[\text{Pt}(\text{triphos})(\text{C}(\text{O})\text{OC}_6\text{H}_4\text{-}p\text{-Me})][\text{PF}_6]$  (**2b**).

first order in  $[\text{CO}]$ , Figures 3 and 4. The reaction shows no observable dependence on the presence of excess aryloxy in solution. The presence of 10, 20, and 40 equiv of aryloxy added to the solution does not affect the rate of the reaction. These observations are consistent with associative kinetics and suggest quite clearly that the carbonylations of **2a--d** do not proceed by a rate-determining dissociation of the aryloxy ligand.

While these observations rule out a dissociative pathway, two associative pathways can still be considered. The first pathway involves classical migratory insertion: axial association of carbon monoxide with the square planar complex followed by insertion into the  $\text{Pt--OAr}$  bond, eq 4. The second pathway

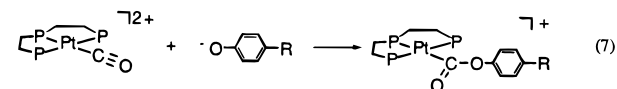
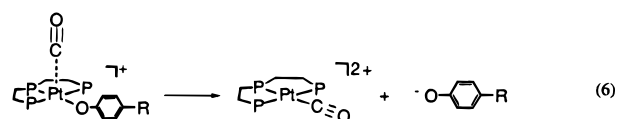
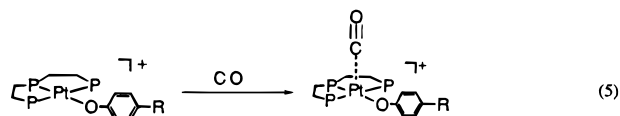


involves an associative substitution of aryloxy for carbon monoxide, eqs 5 and 6, followed by nucleophilic addition of the displaced aryloxy to the coordinated carbon monoxide, eq 7.

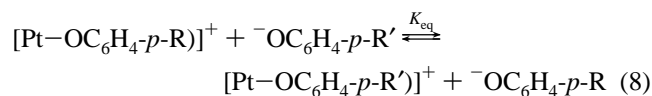
In order to distinguish between the two mechanisms that predict associative kinetics with carbon monoxide, aryloxy ligand exchange and crossover were examined. When 1 equiv of  $\text{NaOC}_6\text{H}_4\text{-}p\text{-R}'$  ( $\text{R}' = \text{OMe}, \text{H}$ ) is added to a solution of  $[\text{Pt}$ -

(51) Allen, F. H.; Kennard, O.; Watson, D. G.; Brammer, L.; Orpen, A. G.; Taylor, R. *J. Chem. Soc., Perkin Trans. 2* **1987**, S1--S19.

(52) Zhong, Z.; Stang, P. J.; Arif, A. M. *Organometallics* **1990**, 9, 1703--1706.



(triphos)(OC<sub>6</sub>H<sub>4</sub>-*p*-Me)[PF<sub>6</sub>] (**2b**), the <sup>31</sup>P{<sup>1</sup>H} NMR shows two products at equilibrium in solution. These two products can be identified as [Pt(triphos)(OC<sub>6</sub>H<sub>4</sub>-*p*-Me)[PF<sub>6</sub>] (**2b**) and [Pt(triphos)(OC<sub>6</sub>H<sub>4</sub>-*p*-R')[PF<sub>6</sub>] (**2a** or **2c**). The reaction is slow enough to enable the observation of two distinct species on the NMR time scale, and the reaction is complete within 20 min. This brackets the rate constant for exchange between 10<sup>2</sup> and 10<sup>-1</sup> s<sup>-1</sup>. These NMR studies also facilitate the measurement of relative stability constants, *K*<sub>eq</sub>, for the different platinum aryloxy complexes **2a–e**, eq 8. Equilibrium constants of 0.75



± 0.2 for the [Pt(triphos)(OC<sub>6</sub>H<sub>4</sub>-*p*-Me)]<sup>+</sup>(**2b**)/[Pt(triphos)(OC<sub>6</sub>H<sub>4</sub>-*p*-OMe)]<sup>+</sup> (**2a**) system, 0.31 ± 0.2 for the [Pt(triphos)(OPh)]<sup>+</sup> (**2c**)/[Pt(triphos)(OC<sub>6</sub>H<sub>4</sub>-*p*-Me)]<sup>+</sup> (**2b**) system, and 0.23 ± 0.2 for the [Pt(triphos)(OPh)]<sup>+</sup> (**2c**)/[Pt(triphos)(OC<sub>6</sub>H<sub>4</sub>-*p*-OMe)]<sup>+</sup> (**2a**) system were obtained. These equilibrium constants favor the platinum aryloxy complexes of the more nucleophilic aryloxy ligands and should be considered within the context of the essentially thermoneutral behavior reported earlier for the exchange of platinum methoxides with methanol.<sup>4</sup> When the equilibrated mixtures of platinum aryloxy complexes are reacted with carbon monoxide at 100 psi, both insertion products appear together at rates seen for the same aryloxy complexes alone. Aryloxy exchange is at least a factor of 1000 times faster than carbon monoxide insertion. Since aryloxy ligand exchange in these systems is so facile, aryloxy displacement by carbon monoxide is also expected to be rapid, eq 6. Thus, unless the presence of carbon monoxide profoundly affects the rate of this exchange, it is difficult to seriously consider aryloxy dissociation as the rate-determining step in the carbonylation of **2a–e**. Inasmuch as square planar ligand substitutions are normally associative, we expect phenoxide exchange to be associative. However, we see no indication that phenoxide inhibits the carbon monoxide insertion reaction. This suggests that the binding of carbon monoxide to the square planar complex is stronger than phenoxide binding. This is to be expected as phenoxide may only donate into a high-energy p orbital, while CO may also interact with the lower energy filled dπ orbitals. The crossover experiment showing that equilibrated mixtures of aryloxy compounds are carbonylated to give both insertion products at the same rates expected for the isolated species is inconsistent with the CO-induced aryloxy dissociative mechanism, eqs 5–7. In the crossover experiment this mechanism would predict preferential dissociation of the better leaving group and nucleophilic addition by the more nucleophilic aryloxy already in solution. The expected result would thus be preferential formation of the insertion product of the more nucleophilic aryloxy, contrary to our experimental observations.

**Table 5.** Pseudo-First-Order Rate Constants for the Carbonylation of the Aryloxy Complexes **2a–d**

compound	<i>k</i> <sub>obs</sub> (× 10 <sup>-4</sup> M <sup>-1</sup> s <sup>-1</sup> )	Hammett <i>σ</i> <sup>47</sup>
[Pt(triphos)(OC <sub>6</sub> H <sub>4</sub> F)][PF <sub>6</sub> ] ( <b>2d</b> )	1.7 ± 0.2	0.06
[Pt(triphos)(OC <sub>6</sub> H <sub>4</sub> H)][PF <sub>6</sub> ] ( <b>2c</b> )	2.3 ± 0.2	0.00
[Pt(triphos)(OC <sub>6</sub> H <sub>4</sub> Me)][PF <sub>6</sub> ] ( <b>2b</b> )	1.3 ± 0.2	-0.17
[Pt(triphos)(OC <sub>6</sub> H <sub>4</sub> OMe)][PF <sub>6</sub> ] ( <b>2a</b> )	1.0 ± 0.2	-0.27

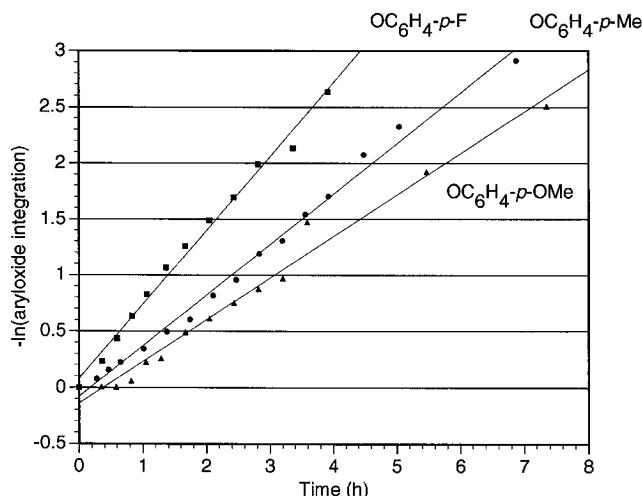


**Figure 5.** Dependence of the observed rate of (aryloxy)carbonyl formation on the aryloxy substituent.

The rate of carbon monoxide insertion is also related to the electronic effects introduced by the *para*-substituents of the aryloxides, Table 5. The rate of carbonylation for the more nucleophilic aryloxides is slower than that for the less nucleophilic aryloxides, Figure 5. These rates also correlate well with Hammett *σ* values.<sup>53</sup> Clearly, the opposite trend would be observed if nucleophilic addition of the displaced aryloxy, eq 7, were the rate-determining step. The presence of excess aryloxy would also affect the rate if nucleophilic addition to coordinated carbon monoxide were rate-determining. This was not observed. These results remove nucleophilic addition of displaced aryloxy to coordinated carbon monoxide, eq 7, as a reasonable rate-determining step. Overall, the facility of aryloxy exchange and relative rates of carbonylation of equilibrated mixtures of different aryloxy complexes together with the *decreased* rates of carbonylation for platinum complexes of *more* nucleophilic aryloxy ligands cannot be reconciled with the carbon monoxide-induced aryloxy dissociation mechanism summarized in eqs 5–7.

The relative stability constants of the aryloxy complexes **2a–c** and the electronic influence of *para*-substituents on the aryloxy ligands both indicate the importance of Pt–O bond breaking in the carbonylation mechanism. When Δ*G*<sup>°</sup>, calculated from the relative stability constants, is compared to Δ*E*<sub>a</sub>, calculated from relative rates for carbonylation, a linear relationship is found. For example, the Δ*G*<sup>°</sup> for the [Pt(triphos)(OPhMe)]<sup>+</sup> (**2b**)/[Pt(triphos)(OPhOMe)]<sup>+</sup> (**2a**) equilibrium is calculated to be 0.71 kJ/mol, and Δ*E*<sub>a</sub> is 0.48 kJ/mol. In the [Pt(triphos)(OPhMe)]<sup>+</sup> (**2b**)/[Pt(triphos)(OPh)]<sup>+</sup> (**2c**) equilibrium, Δ*G*<sup>°</sup> is 2.87 kJ/mol and Δ*E*<sub>a</sub> is 1.52 kJ/mol. Finally for the [Pt(triphos)(OPh)]<sup>+</sup> (**2c**)/[Pt(triphos)(OC<sub>6</sub>H<sub>4</sub>-*p*-OMe)]<sup>+</sup> (**2a**) equilibrium Δ*G*<sup>°</sup> is 3.59 kJ/mol and Δ*E*<sub>a</sub> is 1.99 kJ/mol. This linear free energy relationship suggests that differences in Pt–O bond energy, determined from the relative stability constants,

(53) A plot of the rate of carbon monoxide insertion versus Hammett *σ* gives a best fit line of *k*<sub>obs</sub> = 5.16*σ* + 2.20.

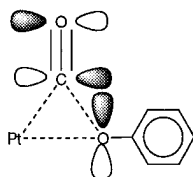


**Figure 6.** Interaction of the carbonyl  $\pi^*$  orbital with the aryloxide oxygen lone pair.

contribute to the activation energy for carbonylation.<sup>54</sup> This supports the notion that Pt–O bond breaking is important in the formation of the transition state. This is further supported by the dependence of the observed rates of carbon monoxide insertion on aryloxide ligand *para*-substitution. More nucleophilic aryloxide ligands are slower to carbonylate since a stronger Pt–O bond must be spent. Together these data support our assertion of a classical migratory insertion pathway, eq 4, for the carbonylation of **2a–e**. While little is known of the structure of the transition state involved and the role of ion solvation energies in the carbonylation of the cationic complexes, our data suggest that differences in Pt–O ground state bond energies are contributed to the differences in activation energies. We note that migratory insertion of carbon monoxide only occurs into the Pt–O bond of Pt(dppe)(Me)(OMe), and not the available Pt–C bond.<sup>38</sup> This preference was attributed to the interaction of the oxygen lone pairs with the carbonyl  $\pi^*$  orbital, Figure 6. Thus, part of the C–O bond is formed

prior to complete Pt–O bond cleavage.<sup>5</sup> This effect would stabilize the transition state and accelerate the rates for the more nucleophilic aryloxides, a trend opposite that observed by us experimentally. We believe that a transition state model like that shown in Figure 6 is sensible for carbonylation of aryloxides, but in our system the influence of Pt–O bond breaking relative to C–O bond making dominates.

It is interesting to note that while we arrive at the same mechanistic conclusion as Bryndza for the carbonylation of platinum aryloxide complexes, the two systems have differing exchange conditions. In the Pt(dppe)(OMe)<sub>2</sub> system, methoxide exchange is found to be slow with respect to insertion.<sup>38</sup> In the aryloxide systems **2a–e**, aryloxide exchange is faster than insertion. In both systems, the mechanism of carbonylation is a classical migratory insertion of the alkyloxide or aryloxide ligand to coordinated carbon monoxide.

**Acknowledgment** is made to the Department of Energy (Grant DE-FG22-93PC93208) and the National Science Foundation (Grant CHE-9319173) for support of this research. We are also grateful to Johnson Matthey for a generous loan of K<sub>2</sub>PtCl<sub>4</sub> and to the NSF for support of the chemical X-ray diffraction facility at Purdue.

**Supporting Information Available:** A plot of  $\Delta E_a$  vs  $\Delta G^\circ$  along with tables of positional and general temperature factors, bond distances, bond angles, and torsional angles, and a description of data collection and reduction for **3b** (26 pages). Ordering information is given on any current masthead page.

JA952680P

(54) A plot of  $\Delta G^\circ$  vs  $\Delta E_a$  gives a best fit line of  $\Delta E_a = 0.55\Delta G^\circ$ ;  $R^2 = 0.994$ .